Journal of Power Sources 271 (2014) 516–521

Contents lists available at ScienceDirect

Journal of Power Sources

journal homepage: www.elsevier.com/locate/jpowsour

Resistance to sulfur poisoning of the gold doped nickel/yttria-stabilized zirconia with interface oxygen vacancy

Yanxing Zhang, Zongxian Yang*

College of Physics and Electronic Engineering, Henan Normal University, Xinxiang, Henan 453007, People's Republic of China

HIGHLIGHTS

- Au dopant prefers to be at the neighbor of the oxygen vacancy site.
- The adsorption and diffusion properties of sulfur on the NiAu-d/YSZ-Ov are studied.
- NiAu-d/YSZ-Ov can weaken the sulfur adsorption at the interface oxygen vacancy.
- NiAu-d/YSZ-Ov can restrain the diffusion of sulfur to the interface oxygen vacancy.

GRAPHICAL ABSTRACT

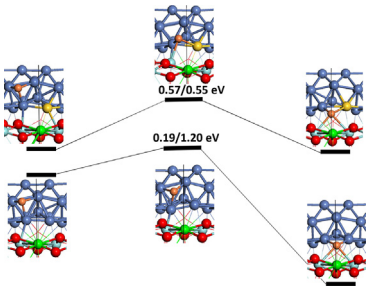

ARTICLE INFO

Article history:
Received 12 May 2014
Received in revised form
26 July 2014
Accepted 3 August 2014
Available online 20 August 2014

Keywords:
Solid oxide fuel cell
Sulfur poisoning
Nickel/yttrium-stabilized zirconia anode
Oxygen vacancy

ABSTRACT

The effects of IB metal (Gold, Silver, and Copper) dopants at the triple phase boundary (TPB) on the resistance to sulfur poisoning of the Nickel/Yttria-Stabilized Zirconia (YSZ) with interface oxygen vacancy (denoted as Ni/YSZ-Ov) are studied using the first-principles method based on density functional theory. Models with Au, Ag, Cu dopants at the TPB of Ni/YSZ-Ov are proposed. It is found that the Au dopant prefers to be at the neighbor of the oxygen vacancy site (denoted as NiAu-d/YSZ-Ov) while the Ag, Cu dopants tend to be located at the top Ni layer, which have little effects on the sulfur adsorption at the interface oxygen vacancy site. Compared with Ni/YSZ-Ov, the NiAu-d/YSZ-Ov can not only weaken the sulfur adsorption at the interface oxygen vacancy site, but also restrain the diffusion of sulfur to the interface oxygen vacancy. Instead, the adsorbed S at the oxygen vacancy is more easily to diffuse out of the interface oxygen vacancy site. So we propose that doping Au in Ni at the neighbor of the interface oxygen vacancy site would be good way to increase the resistance to sulfur poisoning of the Ni/YSZ-Ov anode.

1. Introduction

Solid oxide fuel cells (SOFCs) are expected to be a crucial technology in the future power generation [1,2]. SOFCs offer many desirable advantages compared to other types of fuel cells and conversion devices due to their use of solid electrolytes, lack of moving parts, ability to circumvent precious metal use, high efficiency, low pollution, and fuel flexibility.

The conventional anode for a SOFC is consisted of nickel and yttria-stabilized zirconia (YSZ) (denoted as Ni/YSZ). However, a major issue in the long-term stability and activity of the anode catalyst is its poor resistance toward poisonous compounds presented in the feed stream. Trace amounts of H_2S presented in biomass generated syngas streams are enough to deactivate the catalyst [3,4], which is called sulfur poisoning. Many previous experimental studies indicate that sulfur poisoning behavior is

* Corresponding author.
E-mail addresses: zongxian.yang@163.com, yzx@henannu.edu.cn, yzx@htu.cn (Z. Yang).

http://dx.doi.org/10.1016/j.jpowsour.2014.08.018
0378-7753/

characterized by two stages (fast initial degradation and long term degradation) [4–10].

Liu et al. [7,11] showed that sulfur poisoning observed in the low concentration of H_2S at elevated temperatures is originated from the dissociation of sulfur-containing species and the adsorption of atomic sulfur on the anode surface. The adsorbed H_2S on Ni surfaces has been shown to dissociate above 300 K [12], with only S remaining on the surface. These studies clearly suggest that the elemental sulfur strongly adsorbs on the Ni surfaces with a small activation barrier (E_a) and a large exothermic enthalpy (ΔH). The strongly adsorbed S species block the active sites on the anode surface and thus increase the resistance to electrochemical oxidation of the fuel. The calculations also suggest that the adsorbed sulfur species exist primarily in the form of atomic sulfur instead of molecular species, e.g., H_2S. In fact, the faster or sluggish kinetics is related to the barriers of reactions. The very small E_a means that the barrier for H_2S dissociation is small, but the large exothermic ΔH indicates that the barrier of the reverse reaction of the H_2S dissociation is large. The very small E_a and large exothermic ΔH further imply fast kinetics for sulfur adsorption (as a result of H_2S dissociation) and sluggish kinetics for sulfur removal, which is consistent with the experimental observation of the instant drop in performance upon exposure to H_2S and a very slow recovery in performance after clean hydrogen is switched back. However, experimental results indicated that sulfur tolerance was in fact improved by using Ni/Sc_2O_3 [8] or Ni/Gd_2O_3-doped ZrO_2 [13] anodes, which suggest at least, that sulfur tolerance depends strongly on anode and electrolyte materials besides nickel itself. Zeng et al. [14] have studied the mechanisms governing the sulfur poisoning of the triple-phase boundary (TPB) of Ni/XSZ (X_2O_3 stabilized zirconia) anodes using density functional theory. The calculated sulfur adsorption energies reveal a clear correlation between the size of the cation dopant X^{3+} and the sulfur tolerance of the Ni/XSZ anode. Malyi et al. [15] found that S addition to zirconia, either by doping or through gas diffusion, increases both the formation energy and migration barrier of the oxygen vacancies.

Since the fuel oxidation is believed to take place at the TPB made of Ni, YSZ and fuel gas, which would create oxygen vacancy at the Ni/YSZ interface. As known, the anode of SOFC is the Ni/YSZ composite, instead of the Ni itself. The ideal Ni (111) only represents the anode region beyond the TPB. Therefore, people should give special attention to the Ni/YSZ system and the effects of the interface O vacancy. In our recent work [16], we studied the sulfur poisoning at the TPB region of the Ni/YSZ. We found that the adsorbed sulfur does not favor to be located at the stoichiometric Ni/YSZ interface. With O vacancy at the Ni/YSZ interface, the adsorbed S^- diffuses to the Ni/YSZ interface and is oxidized to S^{2-} and trapped at the oxygen vacancy. The trapped sulfur is very difficult to be removed by the fuel (e.g., H_2) and therefore blocks the pathway for the oxygen ion transfer. As a result, the resistance for oxygen ion transfer would increase and the SOFC performance would drop. Trace amounts of sulfur would block the oxygen vacancy sites at the interface and induce the instant and significant drop in performance of SOFC. To alleviate the sulfur adsorption at the O vacancy site and/or enhance the diffusion of sulfur out of the interface oxygen vacancy site would help to enhance the resistance to sulfur poisoning at the oxygen vacancy site.

To improve the sulfur tolerance of SOFCs, alternative anode compositions have been proposed. Copper/ceria/zirconia [17] anodes were reported to be stable in fuel gases containing up to 450 ppm H_2S. Other anode compositions showing good sulfur tolerance include a lanthanum doped strontium titanate [18], Pd-impregnated titanate/cerate composition [19], lanthanum molybdate [20], gold/molybdenum disulfide [21], Ni/YSZ modified with niobia [22], and lanthanum vanadium oxide [23]. For considerations including cost, processability, and stability, minor modifications to the widely used Ni/YSZ anode may be preferred to the more exotic compositions and forms.

In this work, we focus on the effects of IB metal (Au, Ag, Cu) dopants at the TPB of Ni/YSZ-Ov on the adsorption and the diffusion of sulfur at the interface O vacancy site. We propose that doping Au in Ni at the neighbor of the interface oxygen vacancy site would be good a way to enhance the resistance to sulfur poisoning of the Ni/YSZ-Ov anode.

2. Model and computation method

All calculations presented in this work are performed employing the periodic density functional theory (DFT) method implemented in the Vienna Ab-Initio Simulation Package (VASP) [24]. The exchange–correlation interactions are treated with the Perdew–Burke–Ernzerhof (PBE) functional [25]. Spin-polarized calculations are applied throughout. The electron-ion interactions are treated using the projector augmented wave (PAW) method. [26,27] The wave functions are expanded in plane waves with a cut off energy of 408 eV. The model of the Ni/YSZ cermet with the horizontal dimensions of 12.56 × 7.25 Å as that used in the Shishkin and Ziegler's work [28] is adopted as the substrate. A vacuum layer of 15 Å is used to separate the periodic images in the direction perpendicular to the surface. The model has been successfully used in our previous researches. [16,29,30] In the proposed structure, both Ni and YSZ face each other by the (111) crystallographic planes, with a small lattice mismatch of 3% in the direction with sustained translational symmetry. Experimentally, Abe et al. [31] and other researchers [32,33] fabricated and characterized the Ni/YSZ anode cermet, which has the structure with the (111) planes of the Ni part parallel to the (111) planes of YSZ. Using the transmission electron microscopy technique (TEM), the authors have shown a clear absence of amorphous phases at the interface with a (111)//(111) orientation relationship between Ni and YSZ. The Monkforst-Pack [34] *k*-point mesh of 2 × 3 × 1 is used for the Brillouin zone (BZ) sampling. The atoms in the bottom multilayer are kept fixed for all calculations. Structural optimization of all systems is performed until the atomic forces drop below 0.02 eV $Å^{-1}$. The climbing image nudged elastic band (CI-NEB) [35] method is employed to calculate the transition states and migration barriers. The adsorption energy of a sulfur atom is defined by.

$$E_{ads} = E_S + E_{NiAu-d/YSZ-Ov\ or\ Ni/YSZ-Ov} - E_{S-NiAu-d/YSZ-Ov\ or\ S-Ni/YSZ-Ov} \quad (1)$$

where E_S is the energy of a single S atom simulated in the 8 × 8 × 8 Å box; $E_{S\text{-}NiAu\text{-}d/YSZ\text{-}Ov\ or\ S\text{-}Ni/YSZ\text{-}Ov}$ and $E_{NiAu\text{-}d/YSZ\text{-}Ov\ or\ Ni/YSZ\text{-}Ov}$ are the total energies of NiAu-d/YSZ-Ov or the Ni/YSZ-Ov with and without the S adsorbate, respectively. The $3s^23p^4$ of S, $2s^22p^4$ of O, $3d^84s^2$ of Ni, $5d^{10}6s^1$ of Au, $4d^{10}5s^1$ of Ag, $3d^{10}4s^1$ of Cu, $4d^25s^2$ of Zr and $4s^24p^65s^24d^1$ of Y are treated as valence electrons in the DFT calculations. The Bader charge [36] analysis scheme is applied to determine the atomic charges and charge transfer. Pure GGA functionals underestimate the band gap and, as a consequence, may affect the other properties. This drawback can be remedied in higher levels of theory, e.g. the weighted density approximation (WDA), screened exchange (sX) [37], GW approximation [38], and hybride functionals (HSE06, PBE0, B3LYP) [39,40], etc. However, these methods demand greater computational effort and are not always feasible for large models and extensive sampling. For this reason, in our work we apply the GGA approximation, which is known to give good energetics, and the qualitative description of the electronic structure. We try to use the

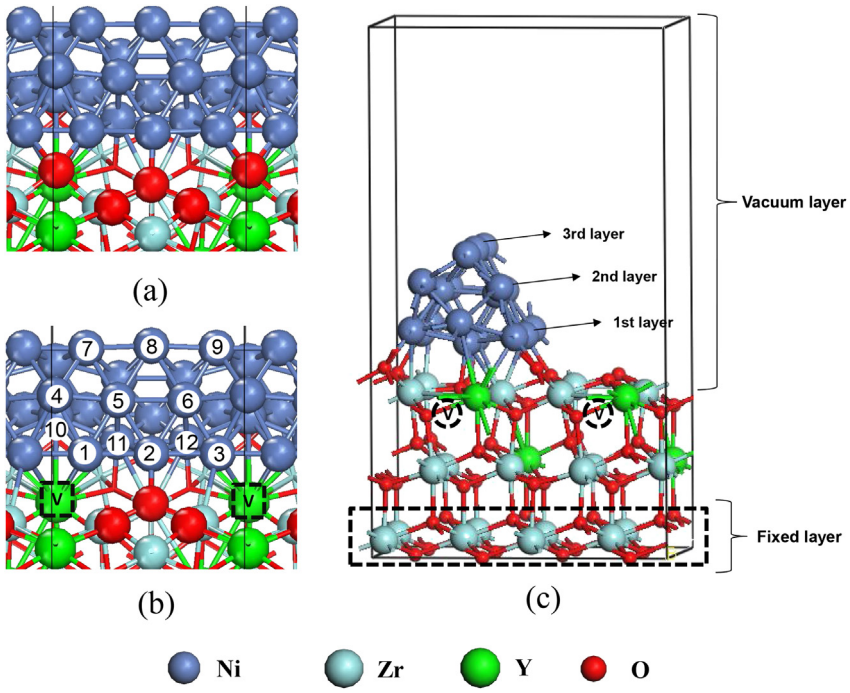

Fig. 1. The Ni/YSZ model: (a), (b) right views, and (c) side views, black dash square in (b) represents the oxygen vacancy at the Ni/YSZ interface, black dash circles in (c) represent the intrinsic oxygen vacancies in the YSZ lattice.

international system of units (SI) in this paper. However, we keep some of the popular units used in the micro world and give their equivalent in SI for clarity, e.g. 1 eV = 1.60217733 × 10^{-19} J; 1 Å = 10^{-10} m; 1 e = 1.60217733 × 10^{-19} C.

3. Results and discussion

3.1. Ni/YSZ-Ov alloyed with Au, Ag, Cu dopants

Firstly, we consider the Ni/YSZ-Ov system alloyed with one Au, Ag or Cu dopant, respectively and test its most stable doping site. Our model contains three Ni layers on YSZ. All the possible doping sites with 12 configurations shown in Fig. 1(b) are considered for the Au, Ag, Cu dopants: three for core, and nine for surface substitutions. The corresponding relative energies of the Au, Ag, and Cu doping systems at different sites are summarized in Table 1. It is found that among the three dopants (Au, Ag, Cu), Au prefers to be at the neighbor (site 1) of the interface oxygen vacancy, while Ag and Cu prefer to be located at the top Ni layer (site 8). Based on the Bader analysis [36], the Au dopant at site 1 gets about 1.07 e, while the Ag (Cu) gets fewer electrons, 0.59 e (0.43 e). From the charge density difference plots of the Au, Ag, Cu doping systems shown in Fig 2(b, d, f), we can see that the dopants get elections not only from the nearby Ni atoms, but also from Zr atoms. The dopants show negative charge and develop static attraction with the neighboring Zr^{4+} cations. The Au dopant has more negative charge, which would develop larger attraction with the cations at the interfaces based on the Coulomb's law. We have also performed test calculations about single Au, Ag, Cu atom adsorption on the surface oxygen vacancy site of YSZ (111) surface. Higher adsorption energy is found for the Au as compared with those for Ag, Cu, (3.77, 2.45 and 2.79 eV for Au, Ag and Cu, respectively), which indicates that the Au has stronger interaction with the Zr. This explains our observation that the Au dopant has larger tendency to be located at the interface site neighboring the oxygen vacancy than the Ag and Cu dopants in the Ni/YSZ-Ov.

Recent studies [41] showed that the strongest effect is observed for the adsorption of sulfur in the vicinity of the alloying atom, whereas, for dopants located far away from alloying atom, the change of binding energies is not observed. Based on our test calculation, we found that with the Ag, Cu dopants at their most stable site (site 8), the sulfur adsorption energies at the interface oxygen vacancy of NiAg(or Cu)-d/YSZ-Ov are 6.16, 6.20 eV, respectively, which are close to the sulfur adsorption energy (6.21 eV) at the interface oxygen vacancy of Ni/YSZ-Ov without Ag, Cu dopants, indicating that the Ag, Cu dopants at the Ni top layer (site 8) have little effects on the sulfur adsorption at the interface oxygen vacancy.

3.2. The adsorption and diffusion of sulfur on the NiAu-d/YSZ-Ov

The model with the Au dopant at site 1 (denoted as NiAu-d/YSZ-Ov) would be the most effective one to affect the S adsorption at the interface oxygen vacancy site compared with the Ag, Cu dopant at

Table 1
The relative energies for the Au, Ag, Cu dopant atom at different sites (the energy of site 1 is set as the reference energy).

Site	**1**	2	3	**4**	5	6	**7**	**8**	**9**	10	11	12
NiAu-d/YSZ-Ov	**0.0**	0.88	0.11	**0.31**	0.83	0.83	**0.25**	**0.02**	**0.23**	1.19	1.70	1.62
NiAg-d/YSZ-Ov	**0.0**	0.50	0.01	**−0.35**	0.34	0.34	**−0.19**	**−0.43**	**−0.20**	0.64	1.69	1.61
NiCu-d/YSZ-Ov	**0.0**	0.23	0.00	**−0.14**	0.16	0.16	**−0.08**	**−0.22**	**−0.08**	0.12	0.29	0.28

Bold values are used to highlight the differences of Au, Ag, Cu dopants at different sites.

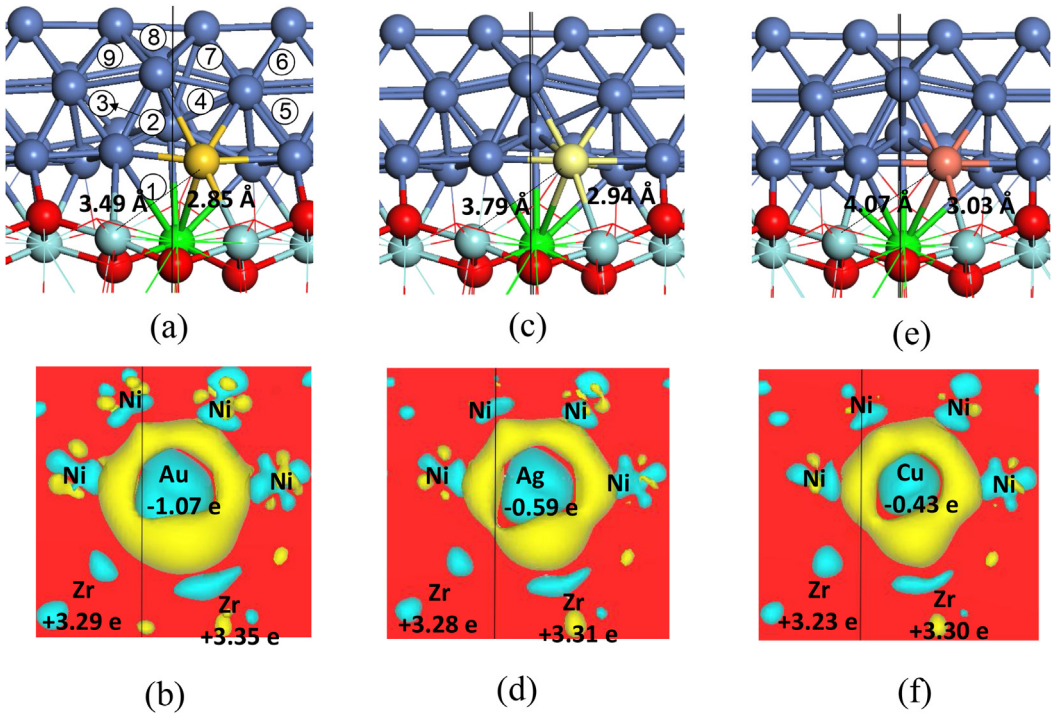

Fig. 2. The NiAu (Ag or Cu)-d/YSZ-Ov systems (a, c, e) and the corresponding charge density difference plots (b, d, f). Negative and positive values are represented in light blue and yellow, respectively. The isosurface value used is 0.02 e/Å^3. (For interpretation of the references to colour in this figure legend, the reader is referred to the web version of this article.)

Table 2
The adsorption properties of sulfur on the NiAu-d/YSZ-Ov. E_{ads}: the adsorption energy of sulfur, the values in the parentheses are the adsorption energy of sulfur on the Ni/YSZ system; $d_{S\text{-}Ni(Zr\ or\ Au)}$: the bond length of the S–Ni(Zr or Au); S-Chg(e): the net charge of the adsorbed sulfur.

	E_{ads}(eV)	$d_{S\text{-}Ni}$(Å)	$d_{S\text{-}Au}$(Å)	$d_{S\text{-}Zr}$(Å)	S-Chg(e)
1	5.13 (6.21)	2.24	2.45	2.60, 2.70	1.18
3	5.11 (5.17)	2.11, 2.17, 2.15		2.64	0.57
4	4.59 (5.08)	2.13, 2.14	2.53		0.54
5	5.00 (4.75)	2.12, 2.11, 2.16			0.52
6	4.96 (4.89)	2.10, 2.11, 2.29			0.54
7	5.25 (5.20)	2.11, 2.14, 2.29			0.61
8	5.33 (5.35)	2.15, 2.16, 2.13			0.61
9	5.11 (5.20)	2.16, 2.18, 2.13			0.57

top of the Ni layer. To this end, we study the adsorption of a sulfur atom on the NiAu-d/YSZ-Ov. The possible S adsorption sites are shown in Fig. 2(a), and the corresponding adsorption energies are summarized in Table 2. The calculation results show that the S adsorption at site 2 is converged to that at site 3. The S atom adsorption energy at the interface oxygen vacancy site is reduced by 1.08 eV compared with that at the interface oxygen vacancy site in Ni/YSZ-Ov. The calculated density of states (DOS) plots of Ni 3d and Au 5d for the atoms at the neighbor of the interface oxygen vacancy site in NiAu-d/YSZ-Ov, as well as that of the corresponding Ni atoms in Ni/YSZ-Ov are shown in Fig. 3. In Fig. 3(a), the Ni atom in NiAu-d/YSZ-Ov gets fewer electrons (0.2 *vs* 0.4 e), showing lower density of states at the Fermi level and lower d band center (−1.55 vs −1.45 eV) than the Ni atom in Ni/YSZ-Ov. In Fig. 3(b), the Au 5d density of states at the Fermi level are much smaller with the

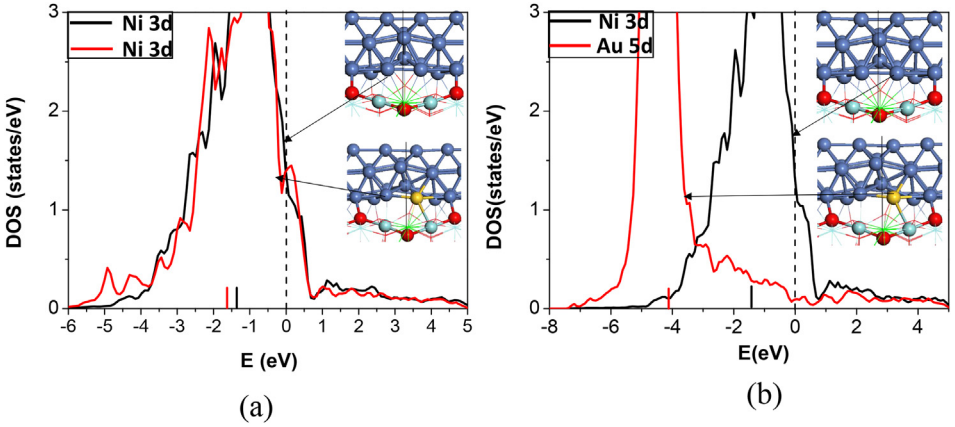

Fig. 3. The density of states (DOS) of Ni 3d at the vacancy site in NiAu-d/YSZ-Ov and Ni/YSZ-Ov (a) and those of Ni 3d in Ni/YSZ-Ov, Au 5d in NiAu -d/YSZ-Ov at the vacancy site (b) (the vertical dash line represents the Fermi level, the vertical short line represents the position of d band center).

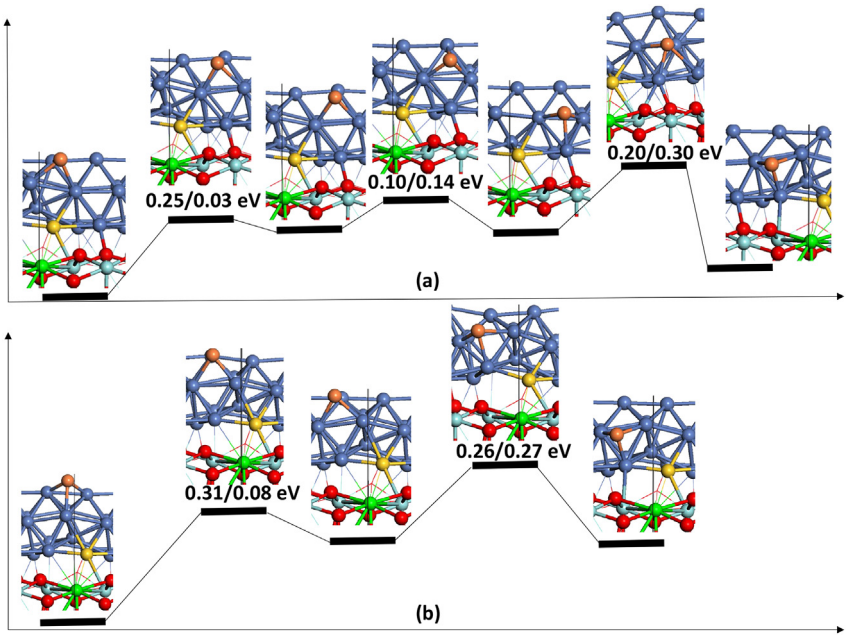

Fig. 4. The MEPs for the different diffusion paths of sulfur on the NiAu -d/YSZ-Ov: (a) "7 → 6 → 5 → 3"; (b) "8 → 9 → 3".

d band center much lower (−4.13 vs −1.43 eV) than those of the Ni atom in Ni/YSZ-Ov. The relative less active Ni and Au atoms in NiAu-d/YSZ-Ov compared with the Ni atoms in Ni/YSZ-Ov accounts for the decreased adsorption energy for the S atom adsorption at the interface O vacancy site.

Of the two nearest adsorption sites to site 1 (sites 3 and 4), the site 3 is much more stable (lower in energy by 0.52 eV) than the site 4. So we select the site 3 as the starting diffusion point of S atom to site 1. We have also calculated the S diffusion paths of '7 → 6 → 5 → 3', and '8 → 9 → 3'. The detailed diffusion paths with the diffusion barriers and geometric structures are shown in Fig. 4(a, b). It is found that the S atom can diffuse easily from sites 5, 6, 7, 8, 9 to site 3 with barriers less than 0.31 eV. The minimum energy paths (MEP) for the diffusion of the adsorbed sulfur atom from site 3 to site 1 in NiAu-d/YSZ-Ov and Ni/YSZ-Ov are shown in Fig. 5. It is found that compared with the sulfur diffusion on the Ni/YSZ-Ov, the sulfur atom is more difficult to diffuse to the interface oxygen vacancy site, with higher activation barrier (0.57 vs 0.19 eV). Instead, the adsorbed S at the oxygen vacancy is easier to diffuse out of the interface oxygen vacancy site, with lower barrier (0.55 vs 1.20 eV). Therefore, the Au dopant at the neighbor of the interface oxygen vacancy site can effectively weaken the S adsorption at the

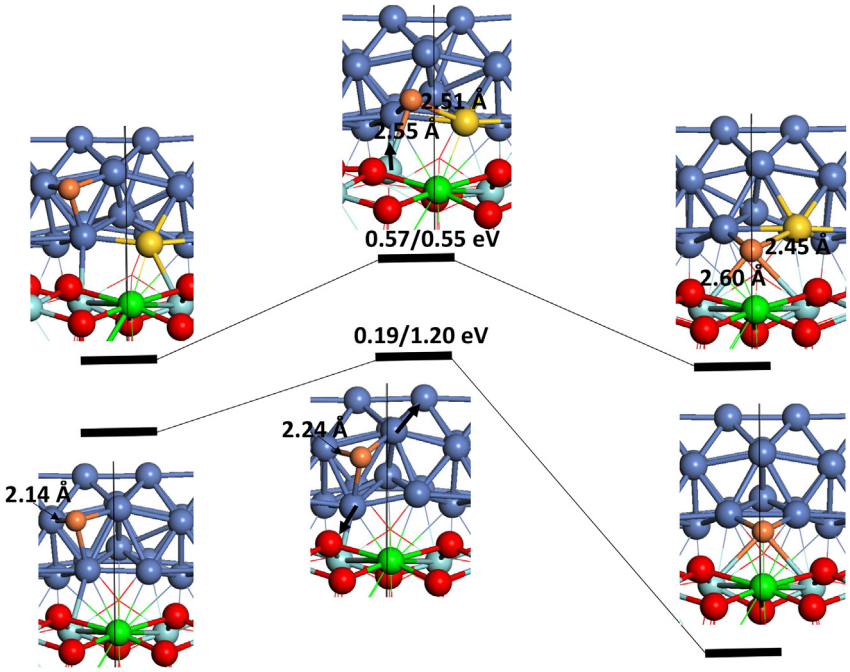

Fig. 5. The MEPs for the different diffusion paths of sulfur on the NiAu -d/YSZ-Ov and Ni/YSZ-Ov.

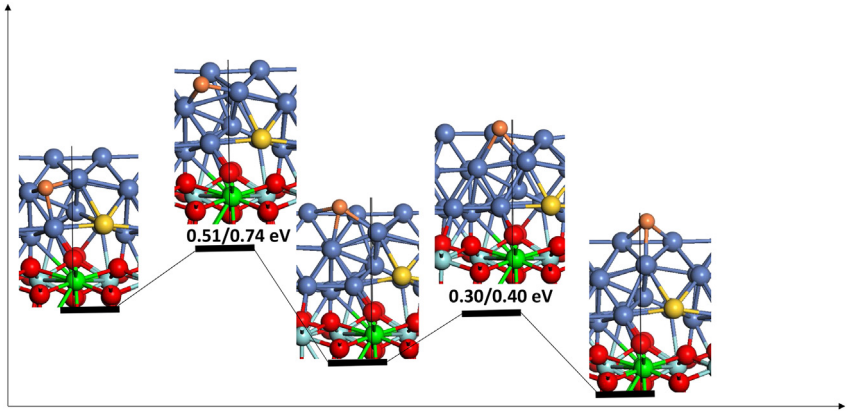

Fig. 6. The MEP for the diffusion path of sulfur on the NiAu-d/YSZ with the interface oxygen vacancy site filled by oxygen.

interface oxygen vacancy site, and restrain the diffusion of sulfur to the vacancy site, which help to enhance the resistance to the sulfur poisoning at the interface oxygen vacancy site. We also calculate the sulfur atom diffusion path when the oxygen vacancy is filled by O. The results shown in Fig. 6 indicate that adsorbed sulfur atom can easily diffuse away from interface oxygen and tends to be located away from the interface.

4. Conclusion

The effects of IB metal (Au, Ag, Cu) dopants at the triple phase boundary on the resistance to sulfur poisoning of the Ni/YSZ with interface oxygen vacancy (denoted as Ni/YSZ-Ov) is studied using the first-principles method based on density functional theory. Models with Au, Ag, Cu dopants at the triple phase boundary of Ni/YSZ-Ov are proposed. It is found that the Au dopant prefers to be at the neighbor of oxygen vacancy site (denoted as NiAu-d/YSZ-Ov), while the Ag, Cu dopants prefers to be at the top Ni layer and have little effects on the sulfur adsorption at the interface oxygen vacancy site. The NiAu-d/YSZ-Ov can not only weaken the sulfur adsorption at the interface oxygen vacancy site, but also restrain the diffusion of sulfur to the interface oxygen vacancy. Instead, the adsorbed S is more easily to diffuse out of the interface oxygen vacancy site. When the interface oxygen vacancy is filled with O atom, the sulfur atom can easily diffuse away from the interface. So we propose that doping Au in Ni at the neighbor of the interface oxygen vacancy site would be a good way to enhance the resistance to sulfur poisoning of the Ni/YSZ-Ov anode.

Acknowledgments

This work was supported by the National Natural Science Foundation of China (Grant No. 11174070) and the Innovation Scientists and Technicians Troop Construction Projects of Henan Province, China (Grant No. 104200510014).

References

[1] R.M. Ormerod, Chem. Soc. Rev. 32 (2003) 17–28.
[2] M.C. Williams, J.P. Strakey, W.A. Surdoval, L.C. Wilson, Solid State Ionics 177 (2006) 2039–2044.
[3] Z. Cheng, J.H. Wang, Y.M. Choi, L. Yang, M. Lin, M. Liu, Energy Environ. Sci. 4 (2011) 4380–4409.
[4] Y. Matsuzaki, I. Yasuda, Solid State Ionics 132 (2000) 261–269.
[5] S. Fang, L. Bi, X. Wu, H. Gao, C. Chen, W. Liu, J. Power Sources 183 (2008) 126–132.
[6] S. Zha, Z. Cheng, M. Liu, J. Electrochem. Soc. 154 (2007) B201–B206.
[7] L. Yang, Z. Cheng, M. Liu, L. Wilson, Energy Environ. Sci. 3 (2010) 1804–1809.
[8] K. Sasaki, K. Susuki, A. Iyoshi, M. Uchimura, N. Imamura, H. Kusaba, Y. Teraoka, H. Fuchino, K. Tsujimoto, Y. Uchida, J. Electrochem. Soc. 153 (2006) A2023–A2029.
[9] Z. Cheng, S. Zha, M. Liu, J. Power Sources 172 (2007) 688–693.
[10] Z. Cheng, M. Liu, Solid State Ionics 178 (2007) 925–935.
[11] J.-H. Wang, M. Liu, Electrochem. Commun. 9 (2007) 2212–2217.
[12] E. Hardegree, P. Ho, J. White, Surf. Sci. 165 (1986) 488–506.
[13] L.L. Zheng, X. Wang, L. Zhang, J.-Y. Wang, S.P. Jiang, Int. J. Hydrogen Energy 37 (2012) 10299–10310.
[14] Z. Zeng, M.E. Bjorketun, S. Ebbesen, M.B. Mogensen, J. Rossmeisl, Phys. Chem. Chem. Phys. 15 (2013) 6769–6772.
[15] O.I. Malyi, P. Wu, V.V. Kulish, K. Bai, Z. Chen, Solid State Ionics 212 (2012) 117–122.
[16] Y. Zhang, Z. Lu, Z. Yang, T. Woo, J. Power Sources 237 (2013) 128–131.
[17] H. He, R.J. Gorte, J.M. Vohs, Electrochem. Solid State Lett. 8 (2005) A279–A280.
[18] R. Mukundan, E.L. Brosha, F.H. Garzon, Electrochem. Solid State Lett. 7 (2004) A5–A7.
[19] X.C. Lu, J.H. Zhu, Z. Yang, G. Xia, J.W. Stevenson, J. Power Sources 192 (2009) 381–384.
[20] X. Lu, J. Zhu, J. Electrochem. Soc. 155 (2008) B1053–B1057.
[21] Z.-R. Xu, J.-L. Luo, K.T. Chuang, J. Power Sources 188 (2009) 458–462.
[22] S. Choi, J. Wang, Z. Cheng, M. Liu, J. Electrochem. Soc. 155 (2008) B449–B454.
[23] L. Aguilar, S. Zha, Z. Cheng, J. Winnick, M. Liu, J. Power Sources 135 (2004) 17–24.
[24] G. Kresse, J. Furthmüller, Phys. Rev. B 54 (1996) 11169.
[25] J.P. Perdew, K. Burke, M. Ernzerhof, Phys. Rev. Lett. 77 (1996) 3865–3868.
[26] P.E. Blöchl, Phys. Rev. B 50 (1994) 17953.
[27] G. Kresse, D. Joubert, Phys. Rev. B 59 (1999) 1758.
[28] M. Shishkin, T. Ziegler, J. Phys. Chem. C 113 (2009) 21667–21678.
[29] Y. Zhang, Z. Fu, S. Dong, Z. Yang, Phys. Chem. Chem. Phys. 16 (2014) 1033–1040.
[30] Y. Zhang, Z. Fu, M. Wang, Z. Yang, J. Power Sources 261 (2014) 136–140.
[31] H. Abe, K. Murata, T. Fukui, W.J. Moon, K. Kaneko, M. Naito, Thin Solid Films 496 (2006) 49–52.
[32] M.C. Muñoz, S. Gallego, J.I. Beltrán, J. Cerdá, Surf. Sci. Rep. 61 (2006) 303–344.
[33] T. Sasaki, K. Matsunaga, H. Ohta, H. Hosono, T. Yamamoto, Y. Ikuhara, Mater. Trans. 45 (2004) 2137–2143.
[34] H.J. Monkhorst, J.D. Pack, Phys. Rev. B 13 (1976) 5188–5192.
[35] G. Henkelman, B.P. Uberuaga, H. Jónsson, J. Chem. Phys. 113 (2000) 9901.
[36] G. Henkelman, A. Arnaldsson, H. Jónsson, Comput. Mater. Sci. 36 (2006) 354–360.
[37] K. Xiong, J. Robertson, M. Gibson, S. Clark, Appl. Phys. Lett. 87 (2005) 183505.
[38] B. Králik, E.K. Chang, S.G. Louie, Phys. Rev. B 57 (1998) 7027.
[39] A. Alkauskas, P. Broqvist, F. Devynck, A. Pasquarello, Phys. Rev. Lett. 101 (2008) 106802.
[40] P. Broqvist, A. Pasquarello, Appl. Phys. Lett. 89 (2006) 262904.
[41] O.I. Malyi, Z. Chen, V.V. Kulish, K. Bai, P. Wu, Appl. Surf. Sci. 264 (2013) 320–328.